

Lithium Enolates Derived from Pyroglutaminol: Aggregation, Solvation, and Atropisomerism

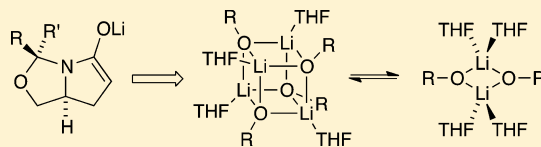
Michael J. Houghton,[†] Naomi A. Biok,[†] Christopher J. Huck,[†] Russell F. Algera,[†] Ivan Keresztes,[†] Stephen W. Wright,[‡] and David B. Collum^{*,†}

[†]Department of Chemistry and Chemical Biology Baker Laboratory, Cornell University Ithaca, New York 14853–1301, United States

[‡]Worldwide Medicinal Chemistry, Pfizer Global Research and Development, 445 Eastern Point Road, Groton, Connecticut 06340, United States

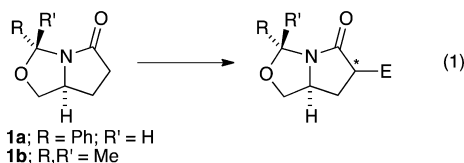
S Supporting Information

ABSTRACT: Lithium enolates derived from protected pyroglutaminols were characterized by using ⁶Li, ¹³C, and ¹⁹F NMR spectroscopies in conjunction with the method of continuous variations. Mixtures of tetrasolvated dimers and tetrasolvated tetramers in different proportions depend on the steric demands of the hemiaminal protecting group, tetrahydrofuran concentration, and the presence or absence of an α -fluoro moiety. The high steric demands of the substituted bicyclo[3.3.0] ring system promote dimers to an unusual extent and allow solvents and atropisomers in cubic tetramers to be observed in the slow-exchange limit. Pyridine used as a ⁶Li chemical shift reagent proved useful in assigning solvation numbers.



INTRODUCTION

As part of a program to develop anti-inflammatory agents, chemists at Pfizer examined functionalizations of readily available protected pyroglutaminols (eq 1).^{1,2} These stereo-



chemically rich, nitrogen-based synthons contain critical features that allow for stereocontrolled functionalizations of both the α and the β carbons. Reactions that exploit the chirality of these compounds include alkylations,^{3,4} aldol and aza-aldol additions,^{5,6} and halogenations^{7,8} of enolates as well as 1,4-additions,^{9,10} cycloadditions,¹¹ dihydroxylations,¹² and cyclopropanations^{13,14} of the analogous α,β -unsaturated lactam. The stereocontrol is often unremarkable; however, compared with the more popular benzylidene analogue **1a**, the acetonide-protected variant **1b** enhances the preference for alkylation from the concave face.^{1,8,15} Given the potential importance of these synthons, surprisingly few variants of the hemiaminal linkage have been reported.¹

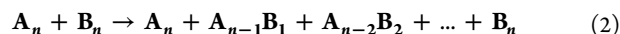
The Cornell contingent was drawn to these protected pyroglutaminols to expand studies of how the aggregation and solvation of lithium enolates influence their reactivities and selectivities.¹⁶ The appeal of the pyroglutaminol-derived skeleton is that the hemiaminal linkage can be varied without perturbing the core γ -lactam moiety. Moreover, the enolate geometries are necessarily *E*, and the chirality provides a means to correlate mechanism and reactivity with stereochemistry.^{17,18}

We describe herein the first of a two-part investigation of lithium enolates **2a–k** and **3–5** (Chart 1) in tetrahydrofuran (THF)/toluene solutions. The deceptively high steric demands stemming from the substituted bicyclo[3.3.0] ring system promote tetramer-to-dimer deaggregation and offer insights into solvation and unexpected atropisomerism within the tetramers. In ongoing studies, we are examining the mechanistic and stereochemical consequences of aggregation and solvation.

RESULTS

Lithium enolates **2–5** were generated from their corresponding lactams¹ by using recrystallized lithium diisopropylamide (LDA, [⁶Li]LDA, or [⁶Li,¹⁵N]LDA).¹⁹ Structures were determined with a combination of ⁶Li NMR spectroscopy, the method of continuous variations (MCV),²⁰ and density functional theory (DFT) calculations at the B3LYP/6-31G(d) level with single-point calculations at the MP2 level of theory.²¹

As a brief reminder, using MCV to characterize aggregates involves mixing two similar enolates, **A_n** and **B_m**, to generate an ensemble of homo- and heteroaggregates (eq 2).^{16,20} The number and symmetries of the heteroaggregates reveal the aggregation state, *n*, which is confirmed by plotting the relative concentrations versus measured²² mole fraction (*X_A* or *X_B*) to generate a Job plot (exemplified by Figures 2 and 4).²³

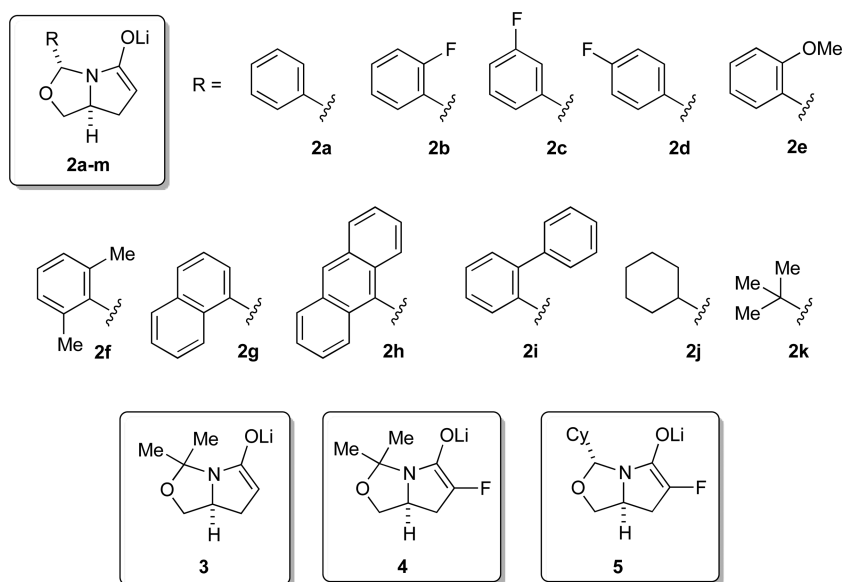


Enolate–LDA Mixed Aggregates in THF. We first addressed the role of LDA mixed aggregates observed when excess LDA is present. For example, generating enolate **3** using excess [⁶Li,¹⁵N]LDA revealed mixed dimer **6** and confirmed

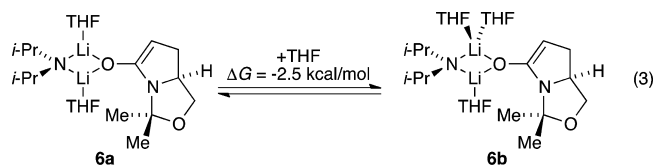
Received: March 2, 2016

Published: April 1, 2016

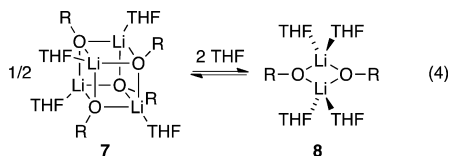
Chart 1



that the structures assigned as enolate hemoaggregates (7 and 8, below) contained no LDA fragments. The mixed dimer **6** displayed the expected ${}^6\text{Li}$ doublet and ${}^{15}\text{N}$ quintet ($J_{\text{Li-N}} = 5 \text{ Hz}$).²⁴ We observed an unusually large THF-concentration-dependent ${}^6\text{Li}$ chemical shift, which suggested that **6** might attain a solvation number >2 . DFT calculations showed some preference for trisolvation over disolvation (eq 3), which is logical given that LDA is a disolvate²⁴ in THF and homodimeric enolates **8** (below) are tetrasolvates.²⁵



Aggregation: Dimer–Tetramer Mixtures in THF/Toluene. ${}^6\text{Li}$ NMR spectroscopy revealed that solutions of enolates **2–5** in THF/toluene solutions afforded two aggregates eventually shown using representative cases to be tetrasolvated tetramers (7) and tetrasolvated dimers (8; eq 4).



The dimers were the only observable form in neat THF. Tetramers became observable typically below 5.0 M THF and were the exclusive form at $<2.0 \text{ M}$ THF. Assignment of the aggregation and solvation states is described below.

With MCV, mixtures of enolates **2b** and **3** in neat THF afforded the two hemoaggregates along with a single heteroaggregate (Figure 1). Monitoring of their proportions versus the measured²² mole fraction provided a Job plot showing a nearly statistical distribution (Figure 2). Dimers derived from **2a,c,e–j** and **3** in neat THF were characterized similarly (Supporting Information).

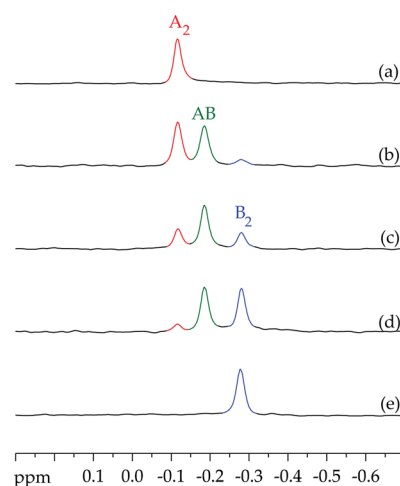


Figure 1. ${}^6\text{Li}$ NMR spectra of 0.10 M solutions of **2b** and **3** in 12.3 M tetrahydrofuran (THF) at $-80 \text{ }^\circ\text{C}$ with 0.13 M $[{}^6\text{Li}]$ LDA (LDA = lithium diisopropylamide). The measured²² mole fractions of **B** (X_{B}) are 0.00, 0.34, 0.54, 0.81, and 1.00 for a–e, respectively.

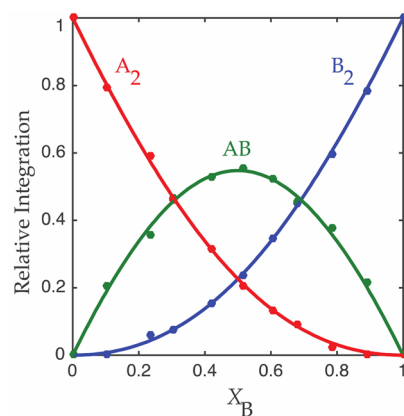


Figure 2. Job plot showing relative integration of the ${}^6\text{Li}$ resonances versus the measured²² mole fraction (X_{B}) of **3** for 0.10 M mixtures of **2b** (A_2) and **3** (B_2) in 12.3 M THF at $-80 \text{ }^\circ\text{C}$.

The higher aggregates observed at low THF concentrations were shown to be tetramers by using MCV on a more select group of enolates. For example, mixtures of enolates **2b** and **3** in 0.13 M total THF concentration (coordinated and free) resulted in mole-fraction-dependent ^6Li spectra consistent with an ensemble of homo- and heteroaggregated tetramers (Figure 3). The resulting Job plot shows a nearly statistical distribution

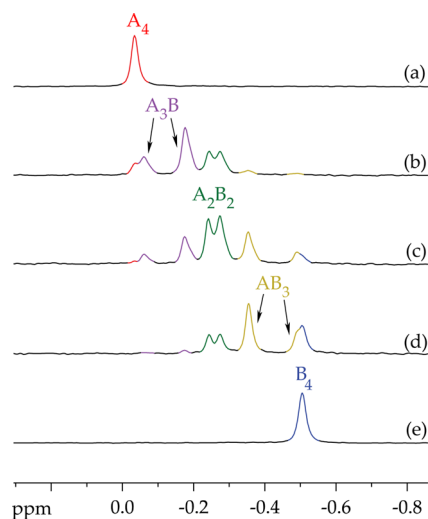


Figure 3. ^6Li NMR spectra of 0.10 M solutions of **2b** and **3** in 0.13 M THF/toluene at $-95\text{ }^\circ\text{C}$ with 0.13 M $[\text{Li}]\text{LDA}$. The measured²² mole fractions of **2b** (X_B) are 0.00, 0.35, 0.52, 0.81, and 1.00 for a–e, respectively.

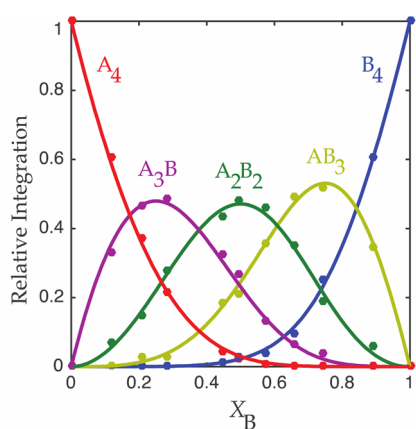


Figure 4. Job plot showing the relative integrations of the ^6Li resonances versus the measured²² mole fractions (X_B) of **2b** for 0.10 M mixtures of **3** (A_2) and **2b** (B_2) in 0.13 M THF/toluene at $-95\text{ }^\circ\text{C}$.

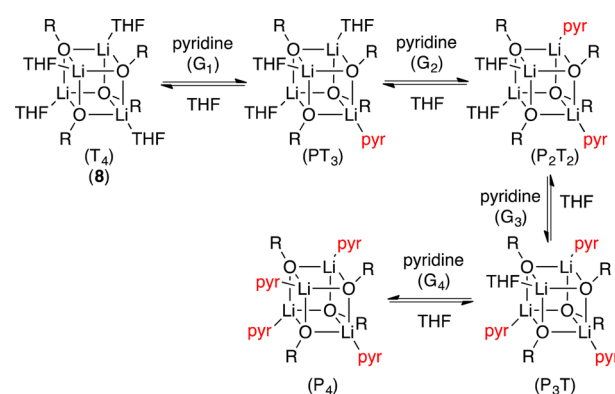
of aggregates (Figure 4). Similar protocols confirmed the higher aggregates of **2i** and **2j** to be tetrameric at low THF concentration (Supporting Information). Enolates **2g** and **2k** also displayed clean ^6Li spectral data and concentration dependencies consistent with tetramer–dimer mixtures, but only the dimers were rigorously characterized. The dependencies on enolate and THF concentration, however, leave little doubt that the tetramers exist in those cases.

As a point of interest in light of efforts to develop MCV for studying nonlithium-based organometallics,¹⁶ mixtures of remotely fluorinated enolates **2b** and **2c** were characterized

with MCV by monitoring well-resolved aggregates using ^{19}F NMR spectroscopy (Supporting Information).^{16,26} The corresponding ^6Li resonances, by contrast, failed to resolve. α -Fluoro enolates **4** and **5** were also characterized with MCV and ^{19}F NMR spectroscopy. The fluorine tag on pairing partner **5** was used to characterize unfluorinated enolate **2j**.

Solvation: Tetramers. It would be reasonable to infer from crystallographic¹⁸ and computational evidence²⁵ that the enolate tetramers are tetrasolvated, as in **8** (Scheme 1), but

Scheme 1



partial solvates have been observed in tetramers comprising hindered enolates.²⁷ To demonstrate qualitatively the existence of solvation, we turned to pyridine as a chemical shift reagent.¹⁶ Incremental additions of pyridine to THF/hydrocarbon solutions of lithium salts left unsolvated nuclei unchanged, whereas resonances corresponding to nuclei bearing substitutionally labile THF ligands shifted markedly downfield.^{16d,e,28}

Incremental replacement of THF by pyridine in 0.10 M solutions of enolate **2j** at $-30\text{ }^\circ\text{C}$, while keeping the total ligand concentration constant (0.50 M), resulted in marked downfield shifts of the observed tetramer. At $-95\text{ }^\circ\text{C}$, however, we detected additional spectral complexity (Figure 5) suggesting that the homo- and heterosolvated tetramers resolved (Scheme

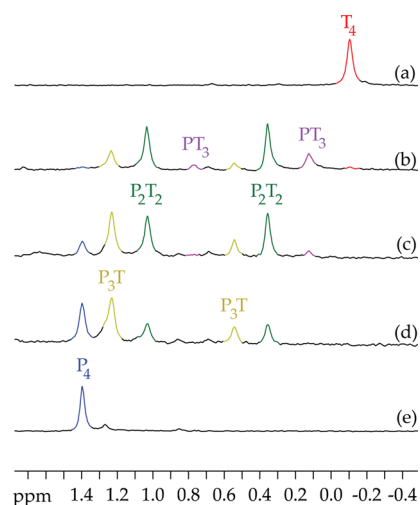


Figure 5. ^6Li NMR spectra of 0.10 M solutions of **2j** in mixtures of THF and pyridine at 0.50 M total concentration with toluene as the cosolvent at $-95\text{ }^\circ\text{C}$ with 0.105 M $[\text{Li}]\text{LDA}$. The measured mole fractions of pyridine (X_P) are 0.00, 0.50, 0.63, 0.75, and 1.00 for a–e, respectively.

1). Also readily apparent were 3:1, 2:2, and 1:3 mixed pyridine–THF solvates. Slow exchange of free and lithium-bound monodentate ligands on NMR time scales is rarely observed²⁹ [with the exception of hexamethylphosphoramide (HMPA)].^{18a,b} [¹⁵N]Pyridine caused the downfield resonances to appear as doublets ($J_{\text{Li-N}} = 4.2\text{--}4.5$ Hz). Monitoring of the proportions of mixed-solvated tetramers versus the measured mole fraction²² (X_{p}) in THF–pyridine mixtures at constant donor ligand concentrations of 0.50 M afforded the relative proportions shown in the Job plot in Figure 6. Finally, varying

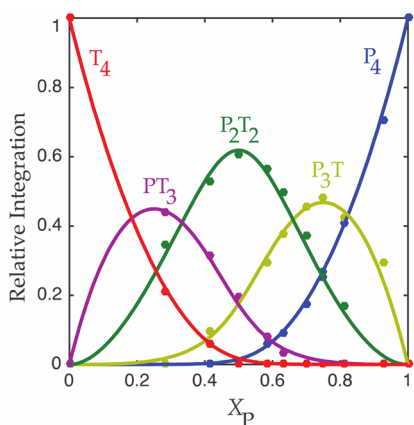


Figure 6. Job plot showing relative integration versus measured mole fraction (X_{p}) of pyridine for 0.50 M total solvent concentration for mixtures of pyridine (P) and THF (T) with 0.10 M **2j** at -95 °C.

the total solvent concentration caused no apparent changes in the coalescence temperature, which indicated that the exchange is dissociative rather than associative.

The Job plot in Figure 6 does *not* attest to the relative binding constants of THF and pyridine because we use the *measured* mole fraction, the mole fraction of only the bound ligands derived from the ⁶Li resonances. Figure 6 shows deviations from a statistical distribution within the bound forms. Gaining insight into the relative binding affinities of THF and pyridine requires a plot of relative integration versus *intended* mole fraction, the actual or total mole fraction of THF and pyridine (Figure 7). A description of the parametric fits is found in the Supporting Information. A discussion of the distortions in Figure 7 and the Job plot in Figure 6 appears below.

Table 1 illustrates the experimentally and computationally determined relative free energies of THF substitution by pyridine. The first row shows the measured free energies extracted directly from the Job plot in Figure 7. Embedded in these numbers are the statistical contributions³⁰ owing to the

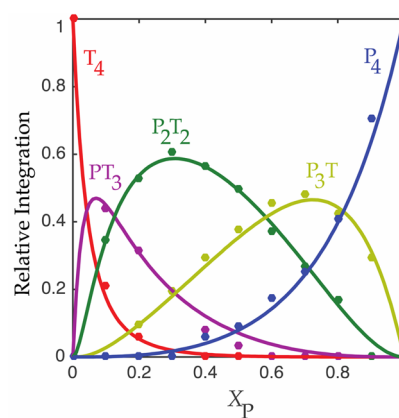


Figure 7. Job plot showing relative integration versus intended (or absolute) mole fraction (X_{p}) of pyridine for 0.50 M total solvent concentration in mixtures of pyridine (P) and THF (T) with 0.10 M **4** at -95 °C.

different numbers of available sites, ranging from four in the fully THF-solvated tetramer to one in the (RO-Li)₄(pyr)₃(THF) tetramer. The second row comprises experimentally measured energies with the statistical factor omitted. The third row corresponds to the DFT-computed energies, which can be directly compared with the statistically corrected experimental numbers. Figure 8 shows a plot of

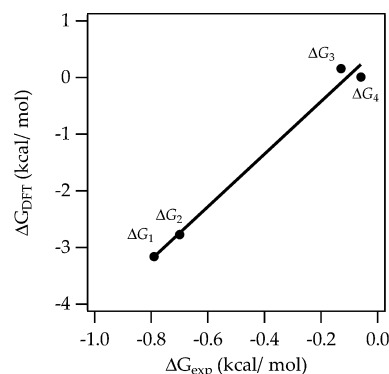


Figure 8. Plot of computed free energies of solvation (ΔG_{DFT} ; from Table 1, row 3) versus statistically corrected experimentally measured free energies of substitution (ΔG_{exp} ; from Table 1, row 2).

theory versus experiment, which would be linear with a slope of unity in the event of a perfect correlation. Because of the skewed distribution of the data, the linearity is correct but unconvincing, and the slope is clearly not unity owing to discrepancies between theory and experiment. The trend, however, is clear.

Table 1. Free Energies of Serial Solvation by Pyridine (See Scheme 1) As Measured Experimentally with the Method of Continuous Variation (See Figure 7) and Computationally with DFT

| | | ΔG_1 | ΔG_2 | ΔG_3 | ΔG_4 |
|----------------------------|--------------------------------------|--------------|--------------|--------------|--------------|
| Experimentally determined | Direct measurement | -1.32 | -0.86 | 0.03 | 0.48 |
| | Statistically ^a corrected | -0.79 | -0.70 | -0.13 | -0.06 |
| Computationally determined | | -3.16 | -2.77 | 0.16 | 0.01 |

^aStatistical correction removes the influence of the number of available sites for substitution, rendering the values directly comparable to the values computed with density functional theory.

We wondered whether the slow exchange in pyridine–THF mixtures arose from strong pyridine binding (akin to HMPA in HMPA–THF mixtures^{18a,b}) and whether THF alone could be observed in the slow-exchange limit. ¹³C NMR spectroscopy of 0.10 M **2j** with 2.25 equiv of THF (total) showed discrete resonances for the α -carbon corresponding to free and bound THF (δ 66.3 and 66.8 ppm, respectively). The approximate 1.3:1 ratio confirmed the 1:1 THF–lithium proportion in the tetramer.

Solvation: Dimers. Addition of pyridine caused a marked (>1.0 ppm) downfield shift of the ⁶Li resonance of the dimer, which confirmed that the dimer was solvated. Confident that the tetramers were tetrasolvates in THF/toluene, we monitored the tetramer–dimer proportions of enolate **3** as a function of THF concentration in toluene (Figure 9 and eq 5). The fit to

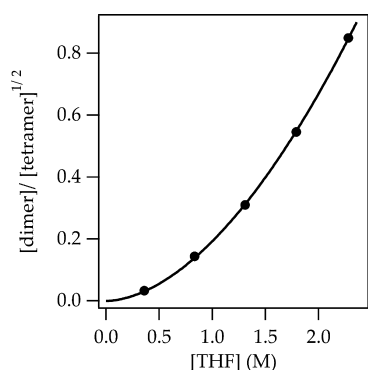


Figure 9. Fit of aggregate relative dimer–tetramer concentrations versus THF concentration for enolate **3** at -80 °C. The curve corresponds to a best fit to $y = k[\text{THF}]^n$ [eq 6; $k = (0.193 \pm 0.002)$, $n = 1.80 \pm 0.02$].

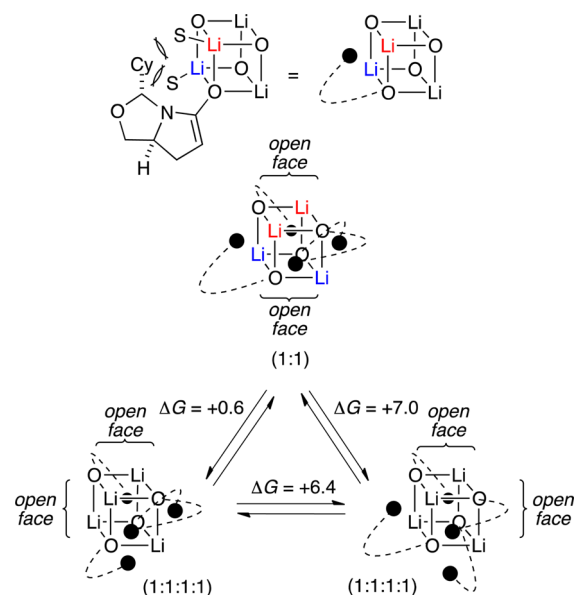
eq 5 (Supporting Information) shows that the dimer is tetrasolvated (eq 6).¹⁸ Analogous THF dependencies were quantitated to show that the dimer of **2j** is also tetrasolvated.³¹



$$[A_2S_{2+n}]/[A_4S_4]^{1/2} = K_{\text{eq}}[S]^n \quad (6)$$

Atropisomerism: Tetramers. Cooling solutions containing exclusively homotetrameric enolate to -120 °C elicited broadening and even multiple resonances in some cases. For example, after cooling, **2j** decoalesced to two broad resonances in a 1:1 proportion. With differential aggregation or solvation excluded as culprits, we were left with rotational isomerism (atropisomerism) arising from restricted rotation around the enolate C–O bonds. Calculations of enolate **2j** show that the cyclohexyl substituents reside over faces of the cube (Scheme 2, top). There are, however, four substituents and six faces, which result in the three possible isomers depicted in Scheme 2. Each face of the cubes that is unencumbered by an enolate substituent is labeled an “open face”. We have also included parenthetically the number of magnetically inequivalent nuclei as well as the relative DFT computed energies (kcal/mol). The computationally preferred atropisomer has an S_4 core structure that would result in the observed 1:1 resonance ratio. A simpler computational model using a methyl rather than a cyclohexyl moiety still showed a preference for the observed high-symmetry atropisomer (Supporting Information). The atropisomer exchange was THF-concentration-independent, con-

Scheme 2



sistent with either a rate-limiting THF dissociation or a mechanism requiring no THF dissociation.

DISCUSSION

Enolates derived from hemiaminal-protected pyroglutaminol have captured the attention of synthetic organic chemists as nitrogen-containing chiral synthons. The differential hindrance of the concave and convex faces offer stereocontrol for further functionalizations. Lithium enolates **2–5** (see Chart 1) are also appealing templates with which to study enolate solvation and aggregation owing to variations available within the hemiaminal linkage that do not invade the inherent γ -lactam local structure.

Aggregation. The deceptively high steric demands of pyroglutaminol-derived enolates **2–5** have a striking impact on aggregation and solvation. Steric effects are notoriously difficult to quantitate because both size and shape are critical. Nonetheless, the hemiaminal substituents that we perceive to be large do indeed promote deaggregation of tetramer to dimer. *tert*-Butyl-substituted enolate **2k**, for example, gives no detectable tetramer with THF concentrations in toluene above 2.0 M, whereas the tetramer of **2a** persists at THF concentrations up to 6.0 M. Compared with their isostructural unfluorinated analogues, the α -fluoro groups on **4** and **5** also promote the dimer by stabilizing the charge. (We observed no evidence of consequential F–Li interactions.)

Solvation. We routinely focus on how ligating solvents determine structure and reactivity. We assigned the tetramers and dimers as tetrasolvates **7** and **8**, respectively, by first showing that tetramer **7** is tetrasolvated and subsequently determining the relative solvation number of dimer **8**.

Assigning the solvation state of tetramer **4a** without merely relying on crystallographic analogy¹⁸ required some luck that began with a simple experiment. We are enamored with the probative role of pyridine as a ⁶Li chemical shift reagent.^{16d,e,28}

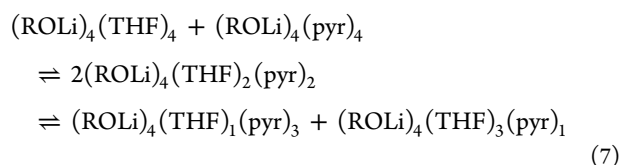
Adding pyridine to THF–toluene solutions of organolithiums results in marked downfield shifts for resonances corresponding to lithium nuclei bearing substitutionally labile THF ligands but has no effect on the chemical shifts of unsolvated ⁶Li nuclei. Of course, in this case we were confident that the ⁶Li nuclei bore at least one coordinated solvent, so it was intended as a control

experiment. We were surprised, however, to observe pyridine–THF mixed solvates in the slow-exchange limit (see Scheme 1): the homo- and heterosolvated tetramers appear as discrete species. The pyridine-solvated nuclei are distinguished by substantial downfield shifts and ^{15}N – ^6Li scalar coupling when [^{15}N]pyridine is used. Besides HMPA–lithium complexes, slow exchange of monodentate ligands on lithium is rarely observed.²⁹ Slow pyridine exchange is *not* merely a consequence of strong coordination by pyridine: free and bound THF can be distinguished on tetramer 2j with ^{13}C NMR spectroscopy, which allowed us to confirm the 1:1 THF–Li stoichiometry.

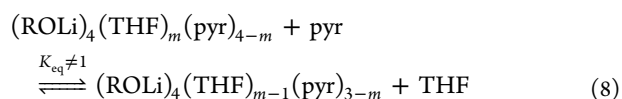
Bolstered by the results from ongoing studies of other enolates,¹⁶ a transiently formed five-coordinate lithium on a tetrameric cube seemed quite plausible.³² The steric hindrance of enolate 2 is critical to slowing the solvent exchange. Solvent-concentration-independent coalescence behavior confirmed what we suspected: solvent substitution is *dissociative*. Given that hindrance should *accelerate* such a dissociative substitution through steric relief,^{29,33} the bulk must suppress otherwise facile associative substitutions. Control experiments showed that less congested enolates such as those derived from indanone undergo rapid THF and pyridine exchange.

Atropisomerism. Cooling solutions of tetramer 7 to -120 °C revealed what we have assigned as atropisomerism. Several of these solutions decoalesce to complex mixtures, whereas others neatly decoalesce to a pair of resonances in a 1:1 ratio. The consequences of restricted rotation about the enolate C–O bonds are highlighted in Scheme 2. The most symmetric form that afforded two resonances is computed to be the most stable (albeit within computational error). We cannot help but see analogy between the shape of enolate 2 and the naphthyl groups in highly restricted binaphthyl moieties. Carlier³⁴ described a series of benzodiazepine-derived enolates in which conformational constraints within a ring had remarkable effects on reactivity. We are unaware of other reports on the atropisomerism of the type described herein,³⁵ but we also cannot currently imagine tangible consequences beyond merely spectroscopic effects.

Comments on MCV. We continue to find applications for MCV (Job plots) in determinations of organolithium structure. A recent review underscores our opinion that such applications reach beyond organolithium chemistry.²⁰ With that said, this study offers an excellent opportunity to emphasize a nuance of Job plots that may be unappreciated by many users, ideas and concerns that mirror those recently articulated by Jurczak and co-workers.³⁶ We use measured mole fraction, the mole fraction determined by integrating all species in the ensemble of aggregates or mixed solvates of a single aggregate, to determine solution structures even on impure samples or when multiple species coexist.¹⁶ For example, Figure 6 shows how pyridine and THF distribute within the ensemble (eq 7) but *provides no insight whatsoever about the relative tendencies of THF and pyridine to bind lithium*. The presence of monomers, dimers, mixed aggregates, and even decomposition does not influence the outcome. Deviations from a statistical distribution reflect only deviations within the ensemble, which make the method robust.



Contrast Figure 6 with Figure 7, in which the absolute mole fraction, the mole fraction dictated by the quantities added, is used. Distortion of the maxima along the x axis toward the lower pyridine mole fractions reflects the higher binding constants of pyridine compared with those of THF. *The analysis was more challenging but achievable because the composition and distribution of all species could be monitored.* It allowed us to extract the binding constants for the sequential substitution of pyridine for THF. The serial substitution by pyridine (see Scheme 1 and eq 8) is progressively less favorable with each substitution. A comparison with the values calculated with DFT (see Table 1 and Figure 8) shows a qualitative correlation that is credible given the inherent limitations of both experiment and theory.



Now we get to the ugly part: *all Job plots are susceptible to this error.* Imagine monitoring species A and B to form adduct A_mB_n . The position of the maximum along the x axis and the curvature reveal the composition of A_mB_n *provided that A_mB_n is the only associated form.* This answer will be quantitatively wrong if there are other undetected equilibria, decompositions, or processes by which the proportions of free A and B are distorted. We escape this trap by monitoring all species within ensembles and using measured mole fractions, but this protocol seems to be rare. One can only imagine how many stoichiometries gleaned from the approximately 6500 studies using MCV²⁰ have been misassigned. It seems almost certain that the answer is not zero.

CONCLUSION

Controlling selectivity is certainly one of the paramount goals of the synthetic organic community. We are currently completing investigations of an aza-aldol addition by pyroglutaminol-derived enolate 2 in which changes in stereoselectivity correlate with changes in mechanism. We are also extending seminal structural studies from the laboratories of Jackman, Seebach, Streitwieser, Williard, Arnett, and Reich (just to name a few)¹⁸ to try to understand if and when tetrameric and dimeric enolates play a role beyond simply being precursors to monomers.³⁷ There is a nagging central question: can one control stereoselectivity by controlling enolate aggregation state? Flowers³⁸ appears to have achieved this goal, but it is a relatively untested hypothesis.

There is a more subtle but noteworthy consequence to the work described herein. The opportunity to observe lithium ion solvation in the slow-exchange limit is not trivial.²⁹ Reich's^{18a,b} studies of HMPA opened an enormous window into solvation as a molecular phenomenon rather than just a medium. Our own experiences with the solvation of lithium hexamethyldisilazide by ethereal solvents in the slow-exchange limit²⁹ were central to our efforts to understand lithium amide structure and reactivity. Gathering hard data on the mechanisms of solvent exchange, relative binding constants, and correlated solvation

within mixed solvates is critical to nudging the chemistry of nondescript lithium salts toward a legitimate subdiscipline of coordination chemistry.

EXPERIMENTAL SECTION

Reagents and Solvents. THF, toluene, and pyridine were distilled from solutions containing sodium benzophenone ketyl. The toluene stills contained approximately 1% tetraglyme to dissolve the ketyl. [⁶Li]LDA and [⁶Li,¹⁵N]LDA were prepared as described previously.¹⁹ Solutions of LDA were titrated for active base with a literature method.³⁹ Air- and moisture-sensitive materials were manipulated under argon with standard glovebox, vacuum line, and syringe techniques.

NMR Spectroscopy. Individual stock solutions of substrates and LDA were prepared at room temperature, and samples of enolate were generated in an NMR tube and flame-sealed as described previously.¹⁶ Standard ⁶Li, ¹³C, ¹⁵N, and ¹⁹F NMR spectra were recorded on a 500 MHz spectrometer at 73.57, 125.79, 50.66, and 470.35 MHz, respectively. The ⁶Li, ¹³C, ¹⁵N, and ¹⁹F resonances were referenced to 0.30 M [⁶Li]LiCl/MeOH at -80 °C (0.0 ppm), the CH₂O resonance of THF at -90 °C (67.57 ppm), neat Me₃NEt at -90 °C (25.7 ppm), and C₆H₅F in neat THF at -80 °C (-112.0 ppm).

Known compounds were prepared according to the literature preparations.^{7a,40}

(3*R*,7*aS*)-3-(2-Fluorophenyl)tetrahydro-3*H*,5*H*-pyrrolo[1,2-*c*]oxazol-5-one (1c). L-Pyrroglutaminol (500 mg, 4.34 mmol), *p*-toluenesulfonic acid (18.0 mg, 0.090 mmol), and 2-fluorobenzaldehyde (0.33 mL, 3.08 mmol) were added to a 25 mL round-bottom flask containing toluene (8.3 mL). The round-bottom flask was attached to a Dean–Stark trap containing toluene and freshly activated 3 Å molecular sieves and was brought to reflux for 5 h. The resulting yellow solution was allowed to cool to rt, and then 10 mL of saturated brine solution was added. This mixture was extracted with 3 × 25 mL of Et₂O, and the organic layers were dried over Na₂SO₄ and dried in vacuo. The resulting yellow oil was purified using flash chromatography in Et₂O and rotary evaporated to yield 470 mg (69%) of white solid: *R*_f = 0.34 in 60% ethyl acetate/hexanes; mp 62.9–68.3 °C; ¹H NMR (400 MHz, CDCl₃) δ 7.22 (td, ⁴*J*_{H-F} = 7.5 Hz, *J*_{H-H} = 7.5, 1.8 Hz, 1H), 7.15 (dddd, ⁴*J*_{H-F} = 5.2 Hz, *J*_{H-H} = 8.0, 7.2, 1.8 Hz, 1H), 6.96 (td, *J* = 7.6, 1.1 Hz, 1H), 6.90 (ddd, ³*J*_{H-F} = 10.5 Hz, *J*_{H-H} = 8.2, 1.1 Hz, 1H), 4.15–3.98 (m, 2H), 3.24 (t, *J* = 7.8 Hz, 1H), 2.59 (ddd, *J* = 17.3, 10.3, 8.8 Hz, 1H), 2.31 (ddd, *J* = 17.3, 10.0, 4.0 Hz, 1H), 2.16 (dddd, *J* = 14.2, 10.1, 7.4, 4.0 Hz, 1H), 1.73 (dddd, *J* = 13.6, 9.9, 8.8, 5.0 Hz, 1H); ¹³C NMR (101 MHz, chloroform-*d*) δ 177.8, 160.5 (d, ¹*J*_{C-F} = 249.3 Hz), 130.4 (d, ³*J*_{C-F} = 8.3 Hz), 127.6 (d, ³*J*_{C-F} = 3.8 Hz), 125.9 (d, ²*J*_{C-F} = 12.7 Hz), 123.8 (d, ⁴*J*_{C-F} = 3.6 Hz), 115.5 (d, ²*J*_{C-F} = 21.0 Hz), 83.4 (d, ³*J*_{C-F} = 2.7 Hz), 71.4, 59.0 (d, ³*J*_{C-F} = 1.0 Hz), 32.9, 22.3; ¹⁹F NMR (376 MHz, CDCl₃) δ -117.20 (ddd, ³*J*_{H-F} = 10.4 Hz, ⁴*J*_{H-F} = 7.4, 5.2 Hz); HRMS (DART ionization, orbitrap mass analyzer) calcd for C₁₂H₁₂FNO₂ [M + H] 222.09303, found 222.09248.

(3*R*,7*aS*)-3-(3-Fluorophenyl)tetrahydro-3*H*,5*H*-pyrrolo[1,2-*c*]oxazol-5-one (1d). yield = 75% (721 mg of white solid). *R*_f = 0.33 in 60% ethyl acetate/hexanes; ¹H NMR (500 MHz, CDCl₃) δ 7.31 (td, ⁴*J*_{H-F} = 5.7 Hz, *J*_{H-H} = 7.9, 5.7 Hz, 1H), 7.23 (ddt, ⁵*J*_{H-F} = 0.9 Hz, *J*_{H-H} = 7.7, 1.7, 0.9 Hz, 1H), 7.14 (dt, ³*J*_{H-F} = 9.6 Hz, *J*_{H-H} = 2.1 Hz, 1H), 6.99 (tdd, ³*J*_{H-F} = 8.4, *J*_{H-H} = 8.4, 2.6, 1.0 Hz, 1H), 6.28 (s, 1H), 4.22 (dd, *J* = 8.1, 6.3 Hz, 1H), 4.14–4.08 (m, 1H), 3.48 (t, *J* = 8.2 Hz, 1H), 2.80 (ddd, *J* = 17.3, 10.2, 9.0 Hz, 1H), 2.54 (ddd, *J* = 17.4, 10.0, 3.8 Hz, 1H), 2.38 (dddd, *J* = 14.1, 10.2, 7.6, 3.8 Hz, 1H), 1.94 (dddd, *J* = 13.3, 9.9, 8.9, 5.4 Hz, 1H); ¹³C NMR (126 MHz, chloroform-*d*) δ 178.2, 162.8 (d, ¹*J*_{C-F} = 246.4 Hz), 141.5 (d, ³*J*_{C-F} = 6.8 Hz), 130.1 (d, ³*J*_{C-F} = 8.0 Hz), 121.7 (d, ⁴*J*_{C-F} = 3.0 Hz), 115.4 (d, ²*J*_{C-F} = 21.2 Hz), 113.0 (d, ²*J*_{C-F} = 22.7 Hz), 86.3 (d, ⁴*J*_{C-F} = 2.2 Hz), 71.7, 58.7, 33.3, 23.0; ¹⁹F NMR (376 MHz, CDCl₃) δ -112.79 (dddd, ³*J*_{H-F} = 9.6 Hz, ³*J*_{H-F} = 8.6 Hz, ⁴*J*_{H-F} = 5.7 Hz, ⁵*J*_{H-F} = 0.9 Hz); HRMS (DART ionization, orbitrap mass analyzer) calcd for C₁₂H₁₂FNO₂ [M + H] 222.09303, found 222.09248.

(3*R*,7*aS*)-3-(2-Methoxyphenyl)tetrahydro-3*H*,5*H*-pyrrolo[1,2-*c*]oxazol-5-one (1e). yield = 24% (486 mg of white solid); *R*_f = 0.21 in 0.34 in 60% ethyl acetate/hexanes; mp 94.5–101.6 °C; ¹H NMR (400 MHz, CDCl₃) δ 7.31 (td, *J* = 7.8, 1.7 Hz, 1H), 7.26 (dd, *J* = 7.5, 1.7 Hz, 1H), 4.32 (tt, *J* = 7.9, 5.7 Hz, 1H), 4.21 (dd, *J* = 8.1, 6.2 Hz, 1H), 3.88 (s, 3H), 3.46 (t, *J* = 8.2 Hz, 1H), 2.85 (dt, *J* = 17.2, 9.6 Hz, 1H), 2.57 (ddd, *J* = 17.3, 10.0, 3.7 Hz, 1H), 2.42 (dddd, *J* = 13.8, 10.0, 7.6, 3.9 Hz, 1H), 1.96 (dtd, *J* = 18.8, 9.5, 5.4 Hz, 1H); ¹³C NMR (126 MHz, CDCl₃) δ 178.0, 157.7, 130.4, 126.6, 126.2, 120.4, 111.2, 84.6, 71.6, 59.9, 55.9, 33.6, 23.1; HRMS (DART ionization, orbitrap mass analyzer) calcd for C₁₃H₁₅NO₃ [M + H] 234.11302, found 234.11247.

(3*R*,7*aS*)-3-(2,6-Dimethylphenyl)tetrahydro-3*H*,5*H*-pyrrolo[1,2-*c*]oxazol-5-one (1f). yield = 30% (174 mg of white solid); *R*_f = 0.34 in 60% ethyl acetate/hexanes; mp 110.6–112.9 °C; ¹H NMR (400 MHz, CDCl₃) δ 7.10 (t, *J* = 7.5 Hz, 1H), 6.99 (d, *J* = 7.5 Hz, 2H), 6.44 (s, 1H), 4.52–4.43 (m, 1H), 4.40 (dd, *J* = 8.3, 5.7 Hz, 1H), 3.48 (t, *J* = 8.7 Hz, 1H), 2.97–2.83 (m, 1H), 2.49 (s, 8H), 2.38 (dddd, *J* = 12.8, 9.4, 6.9, 1.9 Hz, 1H), 1.95 (dddd, *J* = 12.8, 11.5, 9.5, 7.0 Hz, 1H); ¹³C NMR (126 MHz, CDCl₃) δ 178.0, 157.7, 130.4, 126.6, 126.2, 120.4, 111.2, 84.6, 71.6, 59.9, 55.9, 33.6, 23.1; HRMS (DART ionization, orbitrap mass analyzer) calcd for C₁₄H₁₇NO₂ [M + H] 232.13375, found 232.13321.

(3*R*,7*aS*)-3-(Naphthalen-1-yl)tetrahydro-3*H*,5*H*-pyrrolo[1,2-*c*]oxazol-5-one (1g). yield = 51% (561 mg of tan solid); *R*_f = 0.31 in 60% ethyl acetate/hexanes; mp 154.6–161.3 °C; ¹H NMR (400 MHz, CDCl₃) δ 8.44 (d, *J* = 8.4 Hz, 1H), 7.85 (dd, *J* = 12.0, 8.1 Hz, 2H), 7.58 (td, *J* = 6.8, 6.1, 2.2 Hz, 2H), 7.51 (t, *J* = 7.4 Hz, 1H), 7.43 (t, *J* = 7.7 Hz, 1H), 7.06 (s, 1H), 4.29 (t, *J* = 7.2 Hz, 1H), 4.19 (qd, *J* = 7.6, 4.3 Hz, 1H), 3.56 (t, *J* = 8.0 Hz, 1H), 2.84 (ddd, *J* = 17.9, 10.5, 7.6 Hz, 1H), 2.62 (ddd, *J* = 17.6, 10.1, 4.9 Hz, 1H), 2.40 (dddd, *J* = 12.9, 10.3, 7.7, 4.9 Hz, 1H), 2.00 (dddd, *J* = 14.0, 10.0, 7.7, 4.3 Hz, 1H); ¹³C NMR (126 MHz, CDCl₃) δ 179.0, 134.0, 133.7, 130.9, 129.6, 128.6, 126.7, 126.1, 125.0, 124.2, 122.8, 86.2, 71.3, 58.8, 32.8, 22.3; HRMS (DART ionization, orbitrap mass analyzer) calcd for C₁₆H₁₅NO₂ [M + H] 254.11810, found 254.11756.

(3*R*,7*aS*)-3-(Anthracen-9-yl)tetrahydro-3*H*,5*H*-pyrrolo[1,2-*c*]oxazol-5-one (1h). yield = 10% (26.4 mg of yellow solid); *R*_f = 0.23 in 60% ethyl acetate/hexanes; ¹H NMR (500 MHz, CDCl₃) δ 8.63 (dd, *J* = 9.1, 1.1 Hz, 1H), 8.50 (s, 1H), 8.05–7.97 (m, 1H), 7.56 (s, 1H), 7.54 (ddd, *J* = 9.1, 6.5, 1.5 Hz, 1H), 7.46 (ddd, *J* = 8.4, 6.5, 1.0 Hz, 1H), 4.76 (dq, *J* = 9.2, 6.5 Hz, 1H), 4.58 (dd, *J* = 8.6, 5.8 Hz, 1H), 3.72 (t, *J* = 8.9 Hz, 1H), 2.93 (dt, *J* = 17.0, 10.2 Hz, 1H), 2.60 (ddd, *J* = 17.0, 9.7, 2.7 Hz, 1H), 2.50 (dddd, *J* = 12.9, 9.9, 7.2, 2.7 Hz, 1H), 2.09 (dtd, *J* = 13.1, 10.1, 6.4 Hz, 1H); ¹³C NMR (126 MHz, CDCl₃) δ 178.4, 131.7, 130.5, 130.4, 129.5, 126.7, 126.5, 124.9, 124.1, 86.5, 73.2, 60.8, 34.9, 24.3; HRMS (DART ionization, orbitrap mass analyzer) calcd for C₁₅H₁₅NO₃ [M + H] 304.13375, found 304.13440.

(3*R*,7*aS*)-3-([1,1'-Biphenyl]-2-yl)tetrahydro-3*H*,5*H*-pyrrolo[1,2-*c*]oxazol-5-one (1i). yield = 62% (3.01 g of white solid); *R*_f = 0.33 in 60% ethyl acetate/hexanes; mp 108.8–116.2 °C; ¹H NMR (400 MHz, CDCl₃) δ 7.52–7.46 (m, 2H), 7.45–7.38 (m, 3H), 7.38–7.32 (m, 3H), 7.30–7.23 (m, 1H), 4.29 (dtd, *J* = 8.5, 7.2, 6.0 Hz, 1H), 4.18 (dd, *J* = 8.2, 5.9 Hz, 1H), 3.32 (t, *J* = 8.4 Hz, 1H), 2.45 (ddd, *J* = 17.2, 9.9, 3.1 Hz, 1H), 2.34 (dddd, *J* = 13.1, 10.3, 7.4, 3.1 Hz, 1H), 1.86 (dtd, *J* = 13.2, 9.9, 6.0 Hz, 1H); ¹³C NMR (126 MHz, CDCl₃) δ 177.3, 142.3, 140.2, 135.7, 130.8, 129.9, 128.8, 128.1, 127.7, 127.3, 126.4, 86.3, 71.9, 60.9, 34.2, 23.5; HRMS (DART ionization, orbitrap mass analyzer) calcd for C₁₈H₁₇NO₂ [M + H] 280.13375, found 280.13321.

(3*R*,7*aS*)-3-(1-Cyclohexyl-6-fluorotetrahydro-3*H*,5*H*-pyrrolo[1,2-*c*]oxazol-5-one (1k). Lithium diisopropylamide (279 mg, 2.64 mmol) was dissolved in THF (11 mL) and cooled to -78 °C. To this mixture was added 1j (500 mg, 2.40 mmol) dissolved in THF (10 mL), and the resulting mixture was allowed to stir for 10 min to ensure complete enolization. *N*-Fluorobenzenesulfonamide (983 mg, 3.12 mmol) dissolved in THF (4 mL) was added. After 2 h, the reaction was quenched with pH 7 phosphate buffer (6 mL) and allowed to warm. The mixture was extracted with 3 × 20 mL of EtOAc, dried over Na₂SO₄, and rotary evaporated. The resulting yellow oil was purified using flash chromatography with a 70% diethyl Et₂O/pentane solvent system and rotary evaporated to give an oil that was further

recrystallized from Et₂O/pentane to yield 136 mg (25%) of white solid as a single diastereomer: *R_f* = 0.54 in 60% ethyl acetate/hexanes; mp 68.4–69.7 °C; ¹H NMR (400 MHz, CDCl₃) δ 5.08 (ddd, ²J_{H-F} = 51.9 Hz, *J*_{H-H} = 6.4, 1.5 Hz, 1H), 4.99 (dd, ⁵J_{H-F} = 2.4 Hz, *J*_{H-H} = 5.4 Hz, 1H), 4.26–4.16 (m, 2H), 3.28–3.15 (m, 1H), 2.58–2.40 (m, 1H), 2.17–1.96 (m, 1H), 1.83–1.67 (m, 5H), 1.67–1.52 (m, 2H), 1.30–1.01 (m, 5H); ¹³C NMR (126 MHz, chloroform-*d*) δ 170.4 (d, ²J_{C-F} = 17.0 Hz), 94.1 (d, ¹J_{C-F} = 184.7 Hz), 90.8, 71.9 (d, ³J_{C-F} = 2.4 Hz), 58.0, 42.5 (d, ⁵J_{C-F} = 1.0 Hz), 31.6 (d, ²J_{C-F} = 23.7 Hz), 27.47, 27.36, 26.19, 25.67, 25.61. ¹⁹F NMR (376 MHz, CDCl₃) δ –180.90 to –181.29 (m); HRMS (DART ionization, orbitrap mass analyzer) calcd for C₁₂H₁₈FNO₂ [M + H] 228.13998, found 228.13943.

■ ASSOCIATED CONTENT

Supporting Information

The Supporting Information is available free of charge on the ACS Publications website at DOI: 10.1021/acs.joc.6b00459.

Spectroscopic, kinetic, and computational data and the complete citation for ref 21 (PDF)

■ AUTHOR INFORMATION

Corresponding Author

*E-mail: dbc6@cornell.edu.

Notes

The authors declare no competing financial interest.

■ ACKNOWLEDGMENTS

We thank the National Institutes of Health (GM077167) for support.

■ REFERENCES

- (1) (a) Wright, S. W.; Choi, C.; Chung, S.; Boscoe, B. P.; Drozda, S. E.; Mousseau, J. J.; Trzupke, J. D. *Org. Lett.* **2015**, *17*, 5204. (b) Anderson, D. R.; Bunnage, M. E.; Curran, K. J.; Dehnhardt, C. M.; Gavrin, L. K.; Goldberg, J. A.; Han, S.; Hepworth, D.; Huang, H.-C.; Lee, A.; Lee, K. L.; Lovering, F. E.; Lowe, M. D.; Mathias, J. P.; Papaioannou, N.; Patny, A.; Pierce, B. S.; Saiah, E.; Strohbach, J. W.; Trzupke, J. D.; Vargas, R.; Wang, X.; Wright, S. W.; Zapf, C. W. Bicyclic-Fused Heteroaryl or Aryl Compounds and Their Use as IRAK4 Inhibitors. WO 2015150995, Aug 10, 2015.
- (2) Najera, C.; Yus, M. *Tetrahedron: Asymmetry* **1999**, *10*, 2245.
- (3) (a) Yoshioka, S.; Nagatomo, M.; Inoue, M. *Org. Lett.* **2015**, *17*, 90. (b) Kyle, A. F.; Jakubec, P.; Cockfield, D. M.; Cleator, E.; Skidmore, J.; Dixon, D. J. *Chem. Commun.* **2011**, *47*, 10037. (c) Nagasaka, T.; Imai, T. *Chem. Pharm. Bull.* **1995**, *43*, 1081. (d) Zhang, R.; Brownell, F.; Madalengoitia, J. S. *Tetrahedron Lett.* **1999**, *40*, 2707. (e) Clark, A. J.; Filik, R. P.; Thomas, G. H.; Sherringham, J. *Tetrahedron Lett.* **2013**, *54*, 4094. (f) Cowley, A. R.; Hill, T. J.; Kocis, P.; Moloney, M. G.; Stevenson, R. D.; Thompson, A. L. *Org. Biomol. Chem.* **2011**, *9*, 7042. (g) Jao, E.; Bogen, S.; Saksena, A. K.; Girijavallabhan, V. *Synthesis* **2003**, *17*, 2643. (h) Makino, K.; Shintani, K.; Yamatake, T.; Hara, O.; Hatano, K.; Hamada, Y. *Tetrahedron* **2002**, *58*, 9737. (i) Okamoto, N.; Hara, O.; Makino, K.; Hamada, Y. *Tetrahedron: Asymmetry* **2001**, *12*, 1353. (j) Langlois, N.; Rakotonradany, F. *Tetrahedron* **2000**, *56*, 2437. (k) Gu, L.; Yu, M.; Wu, X.; Zhang, Y.; Zhao, G. *Adv. Synth. Catal.* **2006**, *348*, 2223. (l) Sridhar, J.; Wei, Z. L.; Nowak, I.; Lewin, N. E.; Ayres, J. A.; Pearce, L. V.; Blumberg, P. M.; Kozikowski, A. P. *J. Med. Chem.* **2003**, *46*, 4196. (m) Davies, S. G.; Dixon, D. J.; Doisneau, G. J. M.; Prodder, J. C.; Sangane, H. J. *Tetrahedron: Asymmetry* **2002**, *13*, 647. (n) Langlois, N.; Rakotonradany, F. *Tetrahedron* **2000**, *56*, 2437. (o) Bailey, J. H.; Byfield, A. T. J.; Davis, P. J.; Foster, A. C.; Leech, M.; Moloney, M. G.; Muller, M.; Prout, C. K. *J. Chem. Soc., Perkin Trans.* **2000**, *1*, 1977.
- (4) (a) Qiu, Y. L.; Wang, C.; Peng, X.; Cao, H.; Ying, L.; Gao, X.; Wang, B.; Or, Y. S. Novel Benzimidazole Derivatives. WO

2013052369 A1, Apr 11, 2013. (b) Qiu, Y. L.; Wang, C.; Peng, X.; Cao, H.; Ying, L.; Or, Y. S. Hepatitis c virus inhibitors. US 201110142798 A1, Jun 16, 2011. (c) Borriello, M.; Pucci, S.; Stasi, L. P.; Rovati, L. Cyclic amine derivatives as ep4 receptor antagonists. WO 2013004290 A1, Jan 10, 2013. (d) Dahmann, G.; Fiegen, D.; Fleck, M.; Hoffmann, M.; Klicic, J.; East, S. P.; Napier, Spencer Charles, R.; Scott, J. PCT Int. Appl. 2012101013, Aug 2, 2012. (e) Qian, X.; Chuang, C.; Lu, P. P.; Yao, B.; Lu, Q.; Jiang, H.; Wang, W.; Morgan, B. P.; Morgans, D., Jr. Certain chemical entities, compositions, and methods. WO 2009023193 A1, Feb 19, 2009. (f) Kozikowski, A. P.; Blumberg, P. M.; Hennings, H.; Nowak, I. Protein kinase c modulators, and methods of use thereof. WO 2004007445 A3, Jan 22, 2004.

(5) (a) Beard, M. J.; Bailey, J. H.; Cherry, D. T.; Moloney, M. G.; Shim, S. B.; Statham, K. A.; Bamford, M. J.; Lamont, R. B. *Tetrahedron* **1996**, *52*, 3719. (b) Baldwin, J. E.; Moloney, M. G.; Shim, S. B. *Tetrahedron Lett.* **1991**, *32*, 1379. (c) Starkmann, B. A.; Young, D. W. *J. Chem. Soc., Perkin Trans. 1* **2002**, 725.

(6) (a) Bowler, A. N.; Doyle, P. M.; Hitchcock, P. B.; Young, D. W. *Tetrahedron Lett.* **1991**, *32*, 2679. (b) Avent, A. G.; Bowler, A. N.; Doyle, P. B.; Young, D. W.; Marchand, C. M. *Tetrahedron Lett.* **1992**, *33*, 1509. (c) Anwar, M.; Bailey, J. H.; Dickinson, L. C.; Edwards, H. J.; Goswami, R.; Moloney, M. G. *Org. Biomol. Chem.* **2003**, *1*, 2364.

(7) (a) Konas, D. W.; Coward, J. K. *J. Org. Chem.* **2001**, *66*, 8831. (b) Martinez-Montero, S.; Fernandez, S.; Sanghvi, Y. S.; Theodorakis, E. A.; Detorio, M. A.; Mcbrayer, T. R.; Whitaker, T.; Schinazi, R. F.; Gotor, V.; Ferrero, M. *Bioorg. Med. Chem.* **2012**, *20*, 6885. (c) Doyle, M. P.; Hu, W.; Phillips, I. M.; Moody, C. J.; Pepper, A. G.; Slawin, A. M. Z. *Adv. Synth. Catal.* **2001**, *343*, 112. (d) Konas, D. W.; Coward, J. K. *Org. Lett.* **1999**, *1*, 2105.

(8) (a) Barrett, S. D.; Colombo, J. M.; Germain, B. D.; Kornilov, A.; Kramer, J. B.; Uzieblo, A.; Endres, G. W.; Ciske, F. L.; Owen, T. A.; O'Malley, J. P. Methods of Synthesizing a Difluorolactam Analog. WO 2015009991 A2, Jan 22, 2015. (b) Barrett, S. D.; Colombo, J. M.; Germain, B. D.; Kornilov, A.; Kramer, J. B.; Uzieblo, A. Methods of Synthesizing a Difluorolactam Analog. WO 2014144500 A2, Sep 18, 2014. (c) Barrett, S. D.; Ciske, F. L.; Colombo, J. M.; Endres, G. W.; Germain, B. D.; Kornilov, A.; Kramer, J. B.; Uzieblo, A.; Maxey, K. M. Difluorolactam Compounds as EP4 Receptor-Selective Agonists for Use in the Treatment of EP4-Mediated Disease and Conditions. WO 2014015247 A1, Jan 23, 2014. (d) Doyle, M. P.; Hu, W.; Phillips, I. Lewis Acid Catalysis Using Chiral Metal Complexes. WO 2002045853 A1, Jun 13, 2002. (e) Qian, X.; Chuang, C.; Lu, P. P.; Yao, B.; Lu, Q.; Jiang, H.; Wang, W.; Morgan, B. P.; Morgans, D., Jr. Certain Chemical Entities, Compositions, and Methods. WO 2009023193 A1, Feb 19, 2009.

(9) (a) Hanessian, S.; Ratovelomanana, V. *Synlett* **1990**, 501. (b) Hara, S.; Makino, K.; Hamada, Y. *Tetrahedron* **2004**, *60*, 8031. (c) Okamoto, N.; Hara, O.; Makino, K.; Hamada, Y. *Tetrahedron: Asymmetry* **2001**, *12*, 1353. (d) Endo, A.; Danishefsky, S. J. *J. Am. Chem. Soc.* **2005**, *127*, 8298.

(10) Danishefsky, S.; Endo, A. Synthesis of Salinosporamide A and Analogues Thereof. WO 2006124902, Nov 23, 2006.

(11) (a) Tsujishima, H.; Nakatani, K.; Shimamoto, K.; Shigeri, Y.; Yumoto, N.; Ohfun, Y. *Tetrahedron Lett.* **1998**, *39*, 1193. (b) Bailey, J. H.; Cherry, D. T.; Crapnell, K. M.; Moloney, M. G.; Shim, S. B.; Bamford, M. J.; Lamont, R. B. *Tetrahedron* **1997**, *53*, 11731. (c) Bamford, M. J.; Beard, M.; Cherry, D. T.; Moloney, M. G. *Tetrahedron: Asymmetry* **1995**, *6*, 337.

(12) (a) Cottrell, I. F.; Davis, P. J.; Moloney, M. G. *Tetrahedron: Asymmetry* **2004**, *15*, 1239. (b) Kamath, V. P.; Xue, J.; Juarez-Brambila, J. J.; Morris, P. E. *Tetrahedron Lett.* **2009**, *50*, 5198. (c) Smith, A. B., III; Friestad, J. B.; Emmanuel, B.; Duan, J. J. W.; Hull, K. G.; Iwashima, M.; Qiu, Y.; Spoor, P. G.; Salvator, B. A. *J. Am. Chem. Soc.* **1999**, *121*, 10478.

(13) Zhang, R.; Mamai, A.; Madalengoitia, J. S. *J. Org. Chem.* **1999**, *64*, 547.

- (14) Aissaoui, A.; Gude, M.; Boss, C.; Koberstein, R.; Sifferlen, T.; Trachsel, D.; Lehmann, D. *Trans-3-Aza-Bicyclo[3.1.0]Hexane Derivatives*. WO 200916560 A2, Feb 5, 2009.
- (15) (a) Boyd, D. B.; Foster, B. J.; Hatfield, L. D.; Hornback, W. J.; Jones, N. D.; Munroe, E. J.; Swartzendruber, J. K. *Tetrahedron Lett.* **1986**, *27*, 3457.
- (16) (a) Liou, L. R.; McNeil, A. J.; Ramírez, A.; Toombes, G. E. S.; Gruver, J. M.; Collum, D. B. *J. Am. Chem. Soc.* **2008**, *130*, 4859. (b) De Vries, T. S.; Goswami, A.; Liou, L. R.; Gruver, J. M.; Jayne, E.; Collum, D. B. *J. Am. Chem. Soc.* **2009**, *131*, 13142. (c) Tomasevich, L. L.; Collum, D. B. *J. Org. Chem.* **2013**, *78*, 7498. (d) Tomasevich, L. L.; Collum, D. B. *J. Am. Chem. Soc.* **2014**, *136*, 9710. (e) Tallmadge, E. H.; Collum, D. B. *J. Am. Chem. Soc.* **2015**, *137*, 13087.
- (17) (a) Green, J. R. In *Science of Synthesis*; Georg Thieme Verlag: New York, 2005; Vol. 8a, pp 427–486. (b) Farina, V.; Reeves, J. T.; Senanayake, C. H.; Song, J. J. *Chem. Rev.* **2006**, *106*, 2734. (c) Wu, G.; Huang, M. *Chem. Rev.* **2006**, *106*, 2596.
- (18) (a) Reich, H. J. *Chem. Rev.* **2013**, *113*, 7130. (b) Reich, H. J. *J. Org. Chem.* **2012**, *77*, 5471. (c) Seebach, D. *Angew. Chem., Int. Ed. Engl.* **1988**, *27*, 1624. (d) Braun, M. *Helv. Chim. Acta* **2015**, *98*, 1. (e) Williard, P. G. In *Comprehensive Organic Synthesis*; Trost, B. M., Fleming, I., Eds.; Pergamon: New York, 1991; Vol. 1, Chapter 1.1. (f) Kim, Y.-J.; Streitwieser, A. *Org. Lett.* **2002**, *4*, 573. (g) Jackman, L. M.; Lange, B. C. *Tetrahedron* **1977**, *33*, 2737. (h) Li, D.; Keresztes, I.; Hopson, R.; Williard, P. G. *Acc. Chem. Res.* **2009**, *42*, 270. (i) Zune, C.; Jerome, R. *Prog. Polym. Sci.* **1999**, *24*, 631. (j) Baskaran, D. *Prog. Polym. Sci.* **2003**, *28*, 521. (k) Harrison-Marchand, A.; Mongin, F. *Chem. Rev.* **2013**, *113*, 7470.
- (19) Ma, Y.; Hoepker, A. C.; Gupta, L.; Faggini, M. F.; Collum, D. B. *J. Am. Chem. Soc.* **2010**, *132*, 15610.
- (20) Renny, J. S.; Tomasevich, L. L.; Tallmadge, E. H.; Collum, D. B. *Angew. Chem., Int. Ed.* **2013**, *52*, 11998.
- (21) Frisch, M. J. et al. *GaussianVersion 3.09*, revision A.1; Gaussian, Inc.: Wallingford, CT, 2009.
- (22) The measured mole fraction, the mole fraction within only the ensemble of interest, rather than the intended mole fraction of the enolates added to the samples, eliminates the distorting effects of impurities.
- (23) Job, P. *Ann. Chim.* **1928**, *9*, 113.
- (24) Collum, D. B. *Acc. Chem. Res.* **1993**, *26*, 227.
- (25) For leading references to theoretical studies of O-lithiated species, see: (a) Khartabil, H. K.; Gros, P. C.; Fort, Y.; Ruiz-Lopez, M. F. *J. Org. Chem.* **2008**, *73*, 9393. (b) Streitwieser, A. *J. Mol. Model.* **2006**, *12*, 673. (c) Pratt, L. M.; Streitwieser, A. *J. Org. Chem.* **2003**, *68*, 2830. (d) Pratt, L. M.; Nguyen, S. C.; Thanh, B. T. *J. Org. Chem.* **2008**, *73*, 6086.
- (26) (a) Gakh, Y. G.; Gakh, A. A.; Gronenborn, A. M. *Magn. Reson. Chem.* **2000**, *38*, 551. (b) McGill, C. A.; Nordon, A.; Littlejohn, D. J. *Process Anal. Chem.* **2001**, *6*, 36. (c) Espinet, P.; Albeniz, A. C.; Casares, J. A.; Martinez-Ilarduya, J. M. *Coord. Chem. Rev.* **2008**, *252*, 2180.
- (27) Pospisil, P. J.; Wilson, S. R.; Jacobsen, E. N. *J. Am. Chem. Soc.* **1992**, *114*, 7585.
- (28) (a) Reich, H. J.; Kulicke, K. J. *J. Am. Chem. Soc.* **1996**, *118*, 273. (b) Jackman, L. M.; Chen, X. *J. Am. Chem. Soc.* **1997**, *119*, 8681. (c) Jackman, L. M.; Petrei, M. M.; Smith, B. D. *J. Am. Chem. Soc.* **1991**, *113*, 3451. (d) Jackman, L. M.; DeBrosse, C. W. *J. Am. Chem. Soc.* **1983**, *105*, 4177. (e) Dean, R. K.; Reckling, A. M.; Chen, H.; Dawe, L. N.; Schneider, C. M.; Kozak, C. M. *Dalton Trans.* **2013**, *42*, 3504. (f) Boyle, T. J.; Pedrotty, D. M.; Alam, T. M.; Vick, S. C.; Rodriguez, M. A. *Inorg. Chem.* **2000**, *39*, 5133. (g) See also ref 16c.
- (29) (a) Hilmersson, G.; Davidsson, O. *J. Org. Chem.* **1995**, *60*, 7660. (b) Hilmersson, G.; Ahlberg, P.; Davidsson, O. *J. Am. Chem. Soc.* **1996**, *118*, 3539. (c) Boche, G.; Fraenkel, G.; Cabral, J.; Harms, K.; van Eikema Hommes, N. J. R.; Lohrenz, J.; Marsch, M.; Schleyer, P. v. R. *J. Am. Chem. Soc.* **1992**, *114*, 1562. (d) Lucht, B. L.; Collum, D. B. *Acc. Chem. Res.* **1999**, *32*, 1035.
- (30) Benson, S. W. *J. Am. Chem. Soc.* **1958**, *80*, 5151. For additional leading references to statistical contributions in “redistribution reactions”, see: Fay, R. C.; Lowry, R. N. *Inorg. Chem.* **1974**, *13*, 1309.
- (31) Mixtures of enolate **2b**, **2i**, and **3** solvated by TMEDA in toluene afford ensembles of homo- and heteroaggregates consistent with other data ([Supporting Information](#)).
- (32) (a) Lucht, B. L.; Collum, D. B. *J. Am. Chem. Soc.* **1995**, *117*, 9863. (b) Scheschkewitz, D. *Angew. Chem., Int. Ed.* **2004**, *43*, 2965. (c) Niecke, E.; Nieger, M.; Schmidt, O.; Gudat, D.; Schoeller, W. W. *J. Am. Chem. Soc.* **1999**, *121*, 519. (d) Becker, G.; Eschbach, B.; Mundt, O.; Reti, M.; Niecke, E.; Issberner, K.; Nieger, M.; Thelen, V.; Noth, H.; Waldhor, R.; Schmidt, M. Z. *Anorg. Allg. Chem.* **1998**, *624*, 469. (e) Becker, G.; Schwarz, W.; Seidler, N.; Westerhausen, M. Z. *Anorg. Allg. Chem.* **1992**, *612*, 72. (f) Wang, H.; Wang, H.; Li, H.-W.; Xie, Z. *Organometallics* **2004**, *23*, 875. (g) Xu, X.; Zhang, Z.; Yao, Y.; Zhang, Y.; Shen, Q. *Inorg. Chem.* **2007**, *46*, 9379. (h) Thiele, K.; Gorls, H.; Imhof, W.; Seidel, W. Z. *Anorg. Allg. Chem.* **2002**, *628*, 107. (i) Ramirez, A.; Lobkovsky, E.; Collum, D. B. *J. Am. Chem. Soc.* **2003**, *125*, 15376. (j) Buchalski, P.; Grabowska, I.; Kaminska, E.; Suwinska, K. *Organometallics* **2008**, *27*, 2346.
- (33) Choi, M.-G.; Brown, T. L. *Inorg. Chem.* **1993**, *32*, 1548.
- (34) Hsu, D. C.; Lam, P. C.-H.; Slobodnick, C.; Carlier, P. R. *J. Am. Chem. Soc.* **2009**, *131*, 18168.
- (35) For discussions of conformational equilibrations, see: (a) Clegg, W.; Liddle, S. T.; Snaith, R.; Wheatley, A. E. H. *New J. Chem.* **1998**, *22*, 1323. (b) Boche, G.; Fraenkel, G.; Cabral, J.; Harms, K.; van Eikema Hommes, N. J. R.; Lohrenz, J.; Marsch, M.; Schleyer, P. v. R. *J. Am. Chem. Soc.* **1992**, *114*, 1562. (c) Remenar, J. F.; Lucht, B. L.; Kruglyak, D.; Romesberg, F. E.; Gilchirst, J. H.; Collum, D. B. *J. Org. Chem.* **1997**, *62*, 5748.
- (36) Ulatowski, F.; Dąbrowa, K.; Bałakier, T.; Jurczak, J. *J. Org. Chem.* **2016**, *81*, 1746.
- (37) (a) Yamataka, K.; Yamada, H.; Tomioka, H. In *The Chemistry of Organolithium Compounds*; Rappoport, Z.; Marek, I., Eds.; Wiley: New York, 2004, Vol. 2, p 908. (b) Jackman, L. M.; Lange, B. C. *J. Am. Chem. Soc.* **1981**, *103*, 4494. (c) Streitwieser, A.; Wang, D. Z. *J. Am. Chem. Soc.* **1999**, *121*, 6213. (d) Leung, S. S.-W.; Streitwieser, A. *J. Org. Chem.* **1999**, *64*, 3390. (e) Wang, D. Z.; Kim, Y.-J.; Streitwieser, A. *J. Am. Chem. Soc.* **2000**, *122*, 10754. (f) Streitwieser, A.; Kim, Y.-J.; Wang, D. Z. *Org. Lett.* **2001**, *3*, 2599. (g) Streitwieser, A.; Leung, S. S.-W.; Kim, Y.-J. *Org. Lett.* **1999**, *1*, 145. (h) Abboto, A.; Leung, S. S.-W.; Streitwieser, A.; Kilway, K. V. *J. Am. Chem. Soc.* **1998**, *120*, 10807. (i) Leung, S. S.-W.; Streitwieser, A. *J. Am. Chem. Soc.* **1998**, *120*, 10557. (j) Abu-Hasanayn, F.; Streitwieser, A. *J. Org. Chem.* **1998**, *63*, 2954. (k) Abu-Hasanayn, F.; Streitwieser, A. *J. Am. Chem. Soc.* **1996**, *118*, 8136. (l) Gareyev, R.; Ciula, J. C.; Streitwieser, A. *J. Org. Chem.* **1996**, *61*, 4589. (m) Abu-Hasanayn, F.; Stratakis, M.; Streitwieser, A. *J. Org. Chem.* **1995**, *60*, 4688. (n) Dixon, R. E.; Williams, P. G.; Saljoughian, M.; Long, M. A.; Streitwieser, A. *Magn. Reson. Chem.* **1991**, *29*, 509.
- (38) Casey, B. M.; Flowers, R. A. *J. Am. Chem. Soc.* **2011**, *133*, 11492.
- (39) Kofron, W. G.; Baclawski, L. M. *J. Org. Chem.* **1976**, *41*, 1879.
- (40) (a) Himmelsback, F.; Austel, V.; Pieper, H.; Eisert, W.; Mueller, T.; Weisenberger, J.; Linz, G.; Krueger, G. E. *Cyclic Imino Derivatives, Process for Their Preparation, and Drugs Containing Them*. EP 483667 A2 19920506, 1992. (b) Bodur, C.; Kutuk, O.; Karsli-Uzumbas, G.; Isimjan, T. T.; Harrison, P.; Basaga, H. *PLoS One* **2013**, *8*, e56369.